

Effect of Antimony (Sb) Substitution on Ba-Site of Porous Structured $\text{YBa}_2\text{Cu}_3\text{O}_\delta$ Superconductor

Fariesha Farha Ramli^{1*}, Azhan Hashim²

¹Faculty of Applied Sciences, Universiti Teknologi MARA, Perak Branch, Tapah Campus, Tapah Road, 35400 Perak, Malaysia

²Faculty of Applied Sciences, Universiti Teknologi MARA, Pahang Branch, Jengka Campus, Jengka, 26400 Pahang, Malaysia

*Corresponding author E-mail: farie466@perak.uitm.edu.my

Abstract

The effect of antimony (Sb) substitution on Ba-site of porous structure $\text{YBa}_2\text{Cu}_3\text{O}_\delta$ (YBCO) superconductor was investigated. Polycrystalline sucrose was used to create the open pores in the structure. A series of sample with a nominal composition of $\text{YBa}_{2-x}\text{Sb}_x\text{Cu}_3\text{O}_\delta$ where $x = 0.05, 0.10, 0.15, 0.20, 0.30, 0.40$ and 0.50 were synthesized and characterized using X-ray diffraction (XRD) method, resistivity measurement technique and Scanning Electron Microscopic (SEM) equipment. For porous Sb-doped sample with $x \leq 0.30$, the samples showed metallic behavior above onset critical temperature ($T_{C\text{onset}}$) while semiconducting behavior was shown for $x \geq 0.40$. The optimum Sb concentration was achieved at $x = 0.15$, where $T_{C\text{zero}}$ is 85 K and critical current (J_C) value measured at 70 K is 2.75 A/cm^2 . $T_{C\text{onset}}$ and $T_{C\text{zero}}$ of the sample were suppressed towards higher Sb concentration. High level of Sb concentration resulted in the non-superconducting sample and Sb was not incorporated properly into YBCO system. Generally, the crystallographic structure with 123 phase remains as orthorhombic. But, for Sb doping at $x = 0.30$, the sample exhibits tetragonal structure before the presence of 211 phase with the higher Sb concentration. SEM micrograph for porous sample showed the less dense packing with irregular grain shape compared to the standard sample where the small rounded particles grains that can be clearly seen. It can be summarized that the superconducting properties were attributed mainly by the dopants compared to the porous characteristic.

Keywords: Superconductor; YBCO; Sb substitution; Solid state; Porous.

1. Introduction

The foam superconductor was found accidentally by [1] when he was trying to calibrate a thermometer in his magneto-optical cryostat. YBCO foams having the macroscopic shape of bulk materials, but revealing struts with a small thickness could be effectively used as a resistive element in a superconducting fault current limiter [2]. The resultant porous ceramic body may be used as a superconductive device or it may be ground into particles and dispersed as filler in a binder acting as a plastic agent that can be extruded, molded or otherwise shaped to create a Meissner-effect shield, a cylindrical superconductive bearing or other superconductive structure [3].

Other than polyurethane foam, organic compounds can also be used as fillers to create open porosities [4]. The advantage of using this organic compound is that the sample can be pressed before it goes to the sintering process. The best sample contains 60 vol % of the pores with a T_C of 91 K and has a small superconducting transition of 2-3 K. It was reported that porous YBCO is more susceptible to magnetic field because the magnetic field in the structure did not have to be removed out from the sample, while in high dense YBCO the magnetic field was pushed out during the superconducting transition [5].

Doping of Sb to the Cu sites in YBCO superconducting system $\text{YBa}_2\text{Cu}_{3-x}\text{Sb}_x\text{O}_{7-\delta}$ by furnace cooling method was carried out [6]. $T_{C\text{zero}}$ decreased gradually with increasing of Sb content and when $x = 0.3$, zero resistance was not achieved anymore. $T_{C\text{onset}}$ value also shows a decreasing pattern when Sb content is increased. Above the $T_{C\text{onset}}$ where $0.0 \leq x \leq 0.04$, it exhibits metallic behav-

ior while when $x > 0.04$, semiconducting behavior was observed. In 2001, in [7] had reported the J_C dependence to the Sb doping at Y-sites prepared by a sol-gel method. The results showed all sample have $T_{C\text{zero}}$ around 90.6 K and a small amount of Sb increased the J_C value. The maximum value was achieved around 7% of Sb doping. It was reported that J_C was strongly affected by the fraction of the intergranular material, the shape, size and demagnetization factors of the whole sample and grains, the anisotropy of current between and inside the grains, the flux-pinning properties of granular and intergranular materials. Substitution of Sb on Y sites in YBCO superconducting system was reported by [8]. Doping of Sb^{3+} did not give a major effect on the main crystalline structure but the $T_{C\text{zero}}$ of the sample where $x = 0.1 - 6 \text{ mol } \%$ was decreased i.e.: 84.4 K, 83.1 K, 82.7 K and 81.6 K respectively. Due to the depression of $T_{C\text{zeros}}$, Sb was said to have a moderate effect on the conduction mechanism and magnetic order but has an important role in improving the superconducting phase.

Based on this new idea, this research study is focused on a porous structure YBCO superconductor. It covers the process of making a porous superconductor and its superconducting properties before and after adding impurities to the compound. This study is focused on characterization of porous $\text{YBa}_2\text{Cu}_3\text{O}_\delta$ and porous doped $\text{YBa}_{2-x}\text{Sb}_x\text{Cu}_3\text{O}_\delta$ superconductor by solid state reaction technique where $x = 0.05, 0.10, 0.15, 0.20, 0.30, 0.40$ and 0.50 . Crystalline sucrose was used as a supplementary filler to create open pores on the sample. A standard sample was also prepared as a reference for the superconducting properties of the porous sample. Characterization of the sample includes the phase identification, superconducting critical temperature T_C , critical current density J_C and also

microscopic structure. This paper is additional from the previously published paper [9].

2. Methodology

Powder of Y_2O_3 , $BaCO_3$, and CuO and Sb_2O_3 were mixed based on $YBa_{2-x}Sb_xCu_3O_8$ stoichiometry where $x = 0.00, 0.05, 0.10, 0.15, 0.20, 0.30, 0.40$ and 0.50 . The starting powder was mixed thoroughly in a ball mill for 24 hours and dried out in an oven at $120^\circ C$ for about 6 hours. The powder was presintered at $900^\circ C$ for 5 hours in a box furnace, followed by 2 hours grinding. The powder was then sintered at $950^\circ C$ for 5 hours and reground for another 2 hours. The mixed powder was added with crystalline sucrose (the weight ratio of mixed powder: sucrose is 1.8 g: 0.2 g respectively) to create open pores to the sample and pressed under a pressure reaching 30 MPa to get a disc-shaped pellet. The pressed pellets were heated to $400^\circ C$ for 2 hours to remove out the sucrose [4]. After this stage, the samples were sintered again at $960^\circ C$ for 5 hours. All pellets obtained were characterized, which includes phase and microstructure characterization and also T_C and J_C measurement.

3. Results and Discussion

3.1. XRD Analysis

Fig. 1 shows XRD patterns of porous Sb-doped sample, where $x = 0.00 - x = 0.50$. For pure porous $YBa_2Cu_3O_8$ sample, it was highly single phase 123. By comparing the obtained data with calculated XRD patterns, the sample was determined to have dominant peaks of Y-123 phase. Peaks (003), (013), (110), (005), (113), (020) and (116) are proof of 123 phases and were successfully indexed. Optimum splitting between the regions $31.5^\circ \leq 2\theta \leq 33.5^\circ$ can be clearly observed indicates that it has orthorhombic structures because the region is related to the tetragonal-orthorhombic phase transformation [6]. If a sample exhibit tetragonal structure, the peaks are merged together and the splitting cannot be seen. The sample revealed the absence of additional peaks proved that the sucrose added was completely burned out.

The consistency of peak for pure and porous doped sample can be seen up to $x = 0.15$. The intensity and position of those peaks do not have much different. Splitting between peak (013) and (110) was clearly observed indicate that the orthorhombic symmetry is maintained in the structure and the samples were having 123 phase. On the other hand, peak indexed for sample $x = 0.20 - x = 0.50$ show slight deviation compared to the other samples by determination of some impurities. The impurities that being referred from the Xpert High scores report were identified as $YBa_2SbO_6 + CuO$. As the Sb concentration increase, the intensity of impurity peaks increased and peaks in the region between $31.5^\circ \leq 2\theta \leq 33.5^\circ$ that indicate the splitting were diminished. For the sample $x = 0.40$ and $x = 0.50$, the 211 phase was dominant compared to others that still maintaining the 123 phase. The presence of Sb for $x = 0.30 - 0.50$ in the structure inferred that Sb was not successfully substituted the Ba-site in YBCO system at the higher concentration.

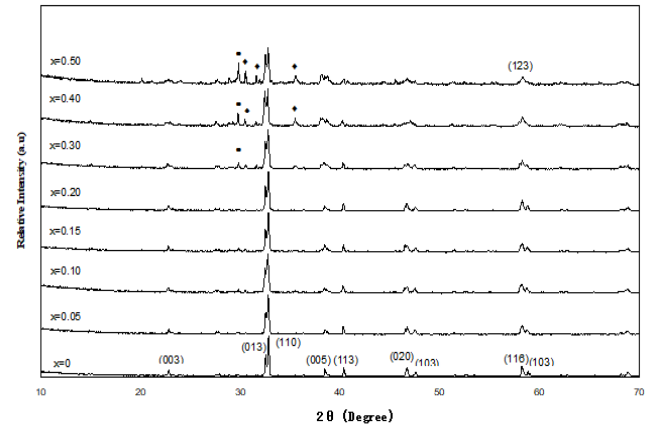


Fig. 1: XRD pattern for pure porous $YBa_2Cu_3O_8$ and porous Sb doped $YBa_{2-x}Sb_xCu_3O_8$ sample (\blacktriangle – $YBa_2SbO_6 + CuO$)

Table 1: Lattice parameter value of standard $YBa_2Cu_3O_8$ and porous Sb-doped sample $YBa_{2-x}Sb_xCu_3O_8$

Sample	a (nm) ± 0.001	b (nm) ± 0.001	c (nm) ± 0.001	Volume (nm) ± 0.003
x = 0.00	0.383	0.389	1.169	0.174
x = 0.05	0.383	0.389	1.168	0.174
x = 0.10	0.383	0.389	1.167	0.174
x = 0.15	0.385	0.388	1.168	0.174
x = 0.20	0.385	0.388	1.166	0.174
x = 0.30	0.386	0.386	1.172	0.175
x = 0.40	0.713	1.218	0.566	0.492
x = 0.50	0.712	1.217	0.565	0.490

Table 1 shows the summarized data of lattice parameter value for samples $x = 0.00 - x = 0.50$. The lattice parameter value supports the XRD patterns as in fig.1 For $x = 0.00 - x = 0.20$, the samples were orthorhombic where $a \neq b \neq c$. While for $x = 0.30$, the sample had changed to the tetragonal where $a = b \neq c$. On the other hand, for $x = 0.40$ and $x = 0.50$, there was a little distortion due to the increase in lattice a and b and a decrease in lattice c parameter. The values proved that both samples were having 211 phase as revealed in Fig. 1.

Sb doping at the higher concentrations where $x = 0.40$ and 0.50 would destroy the dominant 123 phase peak and increase the intensity of impurity, which then leads to the domination of semi-conducting 211 phase. The impurities, YBa_2SbO_6 which a non-superconducting was formed might be due to the partial substitution of Sb to the Cu^{2+} -site due to the almost similar to radius ratio with oxygen which is 0.58 and 0.55 respectively [10]. YBa_2SbO_6 with less oxygen content creates an oxygen deficiency, thus the phenomenon of high- T_C superconductivity clearly disappears. The decreasing of lattice parameter c values at high concentration of Sb may be due to the insertion of Sb with smaller ionic radius (76 pm) to the Ba-site (142 pm) [11]. The same situation also occurs if Ba^{2+} ions are replaced by a smaller ion in YBCO system. The presence of impurity and formation of 211 phase indicates that Ba-site is not favorable for a high concentration of Sb doping because of the large difference in their ionic radius.

3.2. Critical Temperature Measurement (T_C)

Table 2: $T_{C\ onset}$, $T_{C\ zero}$ and ΔT for standard $YBa_2Cu_3O_8$ and porous Sb-doped sample $YBa_{2-x}Sb_xCu_3O_8$

Sample	$T_{C\ onset}$ (K) ± 0.001	$T_{C\ zero}$ (K) ± 0.001	ΔT (K) ± 0.001
Standard YBCO	89	86	3
Porous YBCO	90	85	5
x = 0.05	88	83	5
x = 0.10	90	80	10
x = 0.15	91	85	6
x = 0.20	84	81	3
x = 0.30	86	72	14
x = 0.40	83	-	-
x = 0.50	81	-	-

The value of $T_{C\ onset}$, $T_{C\ zero}$ and difference of $T_{C\ onset}$ and $T_{C\ zero}$, ΔT

for all samples were tabulated in Table 2. The $T_{C\ onset}$ and $T_{C\ zero}$ of the standard and porous pure samples were closely similar, which is about 89 K and 86 K for standard sample and 90 K and 85 K for porous sample respectively. The result shows that the presence of porosity does not enhance or depressed the T_C of the sample. The small ΔT for the standard sample, which is 3 K and having short tails of resistivity indicate the good links between the superconducting grains, while the bigger ΔT for porous sample indicates the separated grains. $T_{C\ onset}$ for $x = 0.05-0.15$ remain almost unchanged which are around 90 K, but the value decreased towards increasing Sb concentration. The highest $T_{C\ zero}$ was observed for sample $x = 0.15$, which is 85 K and decreased as the concentration of Sb increased. At high concentration of Sb where $x = 0.40$ and 0.50 , $T_{C\ zero}$ was not achieved anymore. At a higher concentration of Sb where $x > 0.30$, the superconducting state diminished because of the non-superconducting YBa_2SbO_6 phase, which has a negative effect on the critical temperature [12]. ΔT of the samples varied with Sb concentration and the largest ΔT was observed at $x = 0.30$, which is 14 K. Below the optimum concentration of Sb $x = 0.15$, $T_{C\ zero}$ and $T_{C\ onset}$ were not showing obvious changes which indicate that low concentration of Sb has a moderate effect on the conduction mechanism and also acts as the oxygen stabilizer that maintains the orthorhombicity of the structure. At the high level of Sb doping, depression of T_C maybe because of Ba disorder that might dominate over the oxygen intake which led to the disturbance of orthorhombic symmetry and hence suppresses the T_C [6]. For sample $x = 0.30$ that exhibit the lower $T_{C\ zero}$ might be due to the decreasing of oxygen content $x < 6.4$, thus could be led to the expansion of c axis and become tetragonal structure.

Fig. 2 shows the normalized resistance versus temperature curve for standard $YBa_2Cu_3O_8$ and porous Sb-doped sample $YBa_{2-x}Sb_xCu_3O_8$. It can be observed that standard and porous YBCO samples have a single step superconducting transition with a small width of the superconducting tail. The one step superconducting transition implies that the samples are highly single phase [13]. In this case, the phase was identified as 123 phase. This explanation was supported by the XRD characterization for both samples. Porous sample exhibit lower resistance at normal state compared to the standard sample. Both samples exhibit metallic behavior above the onset temperature. It indicates that both samples are normal conductors before it becomes superconductive.

For porous Sb-doped sample $YBa_{2-x}Sb_xCu_3O_8$, it can be observed that resistivity above $T_{C\ onset}$ for porous doped samples was lower than the standard sample and there was different resistivity among the porous doped sample irrespective of the doping concentration. The transition temperature of the samples varied from 81 to 89 K with the increase in Sb concentration. The graph shows only a one step transition in the normal state. For $x \leq 0.30$ which is 123 phase, it exhibits metallic behavior. While $x = 0.40$ and 0.50 which are 211 phase, it exhibits semiconductor-like behavior.

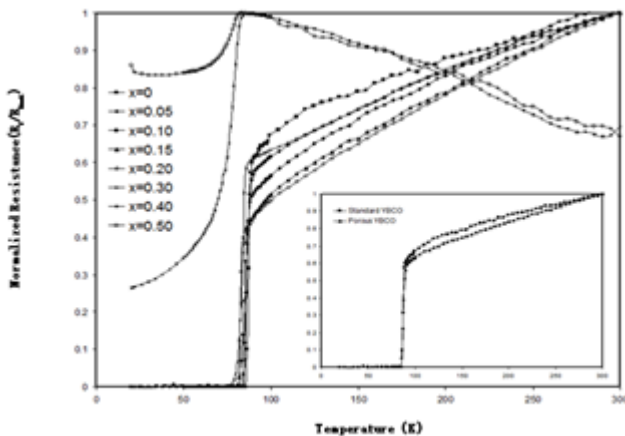


Fig. 2: Normalized resistances versus temperature curve for standard $YBa_2Cu_3O_8$ and porous Sb-doped sample $YBa_{2-x}Sb_xCu_3O_8$

3.3. Critical Current Density Measurement (J_C)

Table 3: J_C value for standard, porous sample and porous Sb-doped sample $YBa_{2-x}Sb_xCu_3O_8$ at 70 K and 60 K

Sample	Critical Current Density (A/cm^2) at $1\mu V$ ± 0.012	
	70 K	60 K
Standard YBCO	6.17	7.67
Porous YBCO	6.33	8.33
$x = 0.00$	6.17	7.67
$x = 0.05$	1.83	2.50
$x = 0.10$	2.25	3.25
$x = 0.15$	2.75	3.42
$x = 0.20$	1.67	2.42
$x = 0.30$	0.33	0.83
$x = 0.40$	-	-
$x = 0.50$	-	-

From values in Table 3, it can be determined that porous sample is having higher J_C compared to the standard sample at 70 K and 60 K even though SEM characterization in Fig. 6 showed that porous sample had separated grains that lead to the weak links. The result is in agreement, which stated the grains boundaries in porous HTS are negligible [14]. In addition, increases of J_C for porous sample might be due to the good electrical contact within the porous ceramic body rather than one just on the surface as in a dense sample [3] and also might be due to the enhancing of pinning due to a fractal structure [15]. For a porous doped sample, it is obviously seen that $x = 0.15$ exhibit the highest J_C but it decreased towards higher Sb concentration. However, J_C values for porous doped samples were lower than the standard sample. This indicates that substitution of Sb to the porous sample cannot overcome weak link behavior that was contributed by inter grain [7]. The fact can be related to the T_C graph that showed wide resistivity tails proving the sample exhibit weak-links. On the other hand, decreases of J_C value may be due to the effect of porous structure. The porous structure could reduce the effective area of current flowing and give the much smaller number of current paths in the porous compared to the dense sample [14]. J_C value for $x = 0.40$ and $x = 0.50$ cannot be measured because they do not superconduct thus do not have superconducting current.

3.4. SEM Characterization

Fig. 3 shows the SEM micrograph for standard sample $YBa_2Cu_3O_8$. It can be observed that the particles were closely packed and are well linked. The sample is considered as homogeneous because no other features are observed. The small rounded particles can be seen clearly in which the crystal orientation of the grains was randomly distributed. While, Fig. 3 shows the SEM picture for porous sample $YBa_2Cu_3O_8$. The sample was determined to be less compact due to the porous structure and also has separated grains. The pores not well distributed because the sucrose was added thoroughly to the mixed powder without a fixed mold, so that the sucrose just randomly distributed into the structure. Besides that, the grains of the sample looked roughened due to the effect of sucrose melting during the heating process and were in irregular shape.

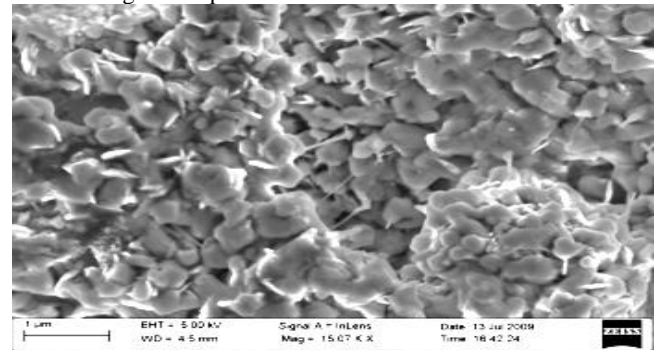


Fig. 3: SEM micrograph of standard sample $YBa_2Cu_3O_8$

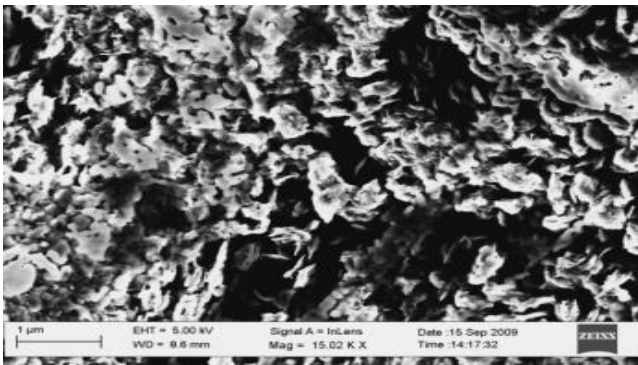


Fig. 4: SEM micrograph of porous sample $\text{YBa}_2\text{Cu}_3\text{O}_8$

Fig. 4 shows the SEM micrograph for porous Sb-doped sample $\text{YBa}_{2-x}\text{Sb}_x\text{Cu}_3\text{O}_8$, for sample $x = 0.05$, it shows the compact structure with large grain particles. The grain size is in the range of $1\mu\text{m}$ to $2\mu\text{m}$ and was in random distribution. The grain boundaries are clearly visible and linked to each other. The structure was considered homogenous because no impurities detected. Doping of Sb at $x = 0.10$ caused the grains to become smaller. The particles are coarse and in crystal-like structure with a less compact arrangement. Pores can be observed clearly showing that the grains are not well linked together. It also shows the irregular grain shape with no specific grain alignment. for $x = 0.15$ and 0.20 , it can be observed that both samples exhibit almost the same microstructure. The grains are of irregular shape and size with less dense packing. The grains particles are distributed randomly without specific alignment and pores can be observed within the structure. Micrograph structure for $x = 0.30$ shows that there is a thin flake-shape lamina stacked on one another. This packing of grains caused the structure look much denser. The very small particles are randomly distributed and seem to be coagulated to form a cluster. For high Sb doping, where $x = 0.40$ and 0.50 show different microstructure. The structure becomes less dense and the grain size is significantly small. The grains particles seem to be coagulated to form clusters and it shows the low connectivity between the grains. The crystal structures are not homogeneous in size or shape, thus failed to pass the levitation test at liquid-nitrogen temperature by means of the Meissner Effect [10]. This observation supports the T_C measurement result, where sample with $x = 0.40$ and 0.50 are not superconductive.

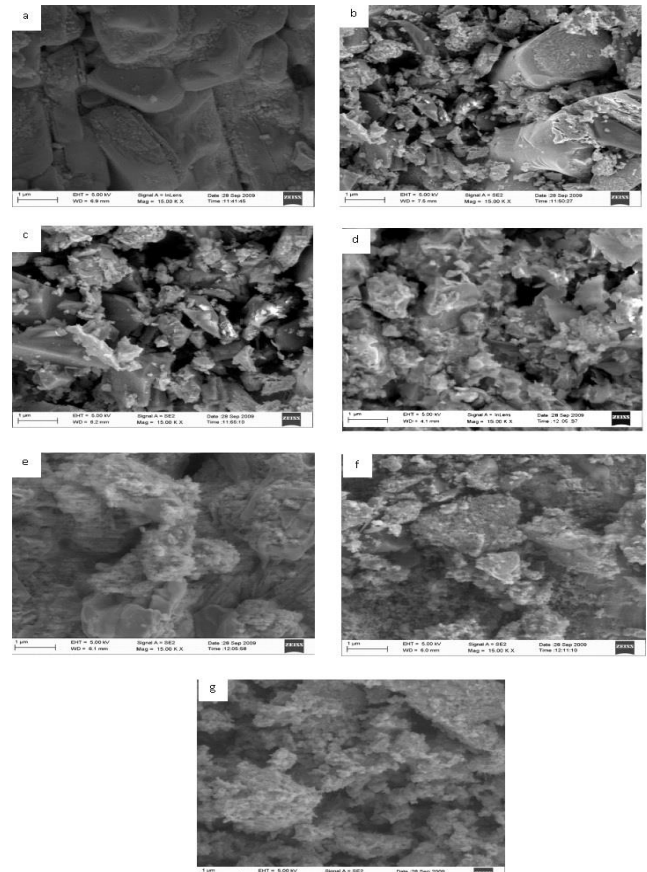


Fig. 5: SEM micrograph for sample a) $x = 0.05$ b) $x = 0.10$ c) $x = 0.15$ d) $x = 0.20$ e) $x = 0.30$ f) $x = 0.40$ and g) $x = 0.50$

4. Conclusion

Undoped and doped porous sample have been successfully synthesized through solid state technique and the superconducting properties of the sample were investigated. From this study, it can be concluded that increasing of T_C and J_C of the porous doped sample may be attributed mainly by the dopants. The porous characteristic does not contribute much to the superconducting properties because there is only a little deviation from the porous and standard sample YBCO. The best superconducting properties for doped sample $\text{YBa}_{2-x}\text{Sb}_x\text{Cu}_3\text{O}_8$ were observed at $x = 0.15$. porous Sb-doped sample, there is no improvement in superconducting properties. All sample exhibit increasing values of T_C and J_C towards the optimum concentration and decrease for further addition of dopants concentration. High level of doping also showed a deviation in XRD peaks, indicating the presence of impurities in the structure. The smaller ionic radius of Sb^{3+} (76 pm) affects to the decrease of the lattice parameter c . Weak links were identified as a factor of which decreases J_C for Sb-doped samples. Sucrose added was completely burnt out and successfully creates open pores to the structure.

Acknowledgement

We would like to acknowledge the financial support granted by Ministry of Higher Education (MOHE) for Research Acculturation Grant Scheme (RAGS) 600-RMI/RAGS 5/3 (146/2014) and UiTM for the facilities provided.

References

- [1] Prozorov, R., Equilibrium Topology of the Intermediate State in Type-I Superconductors of Different Shapes, *Physical Review Letters*, (2007), 98, 1-5.

- [2] Noudem, J. G., Reddy, E. S., Schmitz, G. J., Magnetic and Transport Properties of $\text{YBa}_2\text{Cu}_3\text{O}_y$ Superconductor Foams, *Physica C*. (2003), 390, 286-290.
- [3] Reick, F. G., Westwood, N. J., High-Temperature Porous-Ceramic Superconductors U. S. Patent 4,999,322, (1991).
- [4] Fiertek, P., Sadowski, W., Processing of Porous Structures of $\text{YBa}_2\text{Cu}_3\text{O}_{7-\delta}$ High-Temperature Superconductor, *Materials Science-Poland*, (2006), 24, 1103-1108.
- [5] Fiertek, P., Andrzejewski, B., Sadowski, W., Synthesis and Transport Properties of Porous Superconducting Ceramics of $\text{YBa}_2\text{Cu}_3\text{O}_{7-\delta}$, *Advanced Material Science*, (2010), 23, 52-56.
- [6] Akhtar, M. J., Shaheen, R., Haque, M. N., Bashir J., Akhter, J. I., Synthesis and Characterization of $\text{YBa}_2\text{Cu}_{3-x}\text{Sb}_x\text{O}_{7-\delta}$ High-Temperature Superconductors, *Superconductor Science and Technology*, (2000), 13, 1612-1620.
- [7] Botelho, D.F., Lisboa-Filho, P. N., Araujo-Moreira, F. M., Bulk Critical Current Density Dependence on the Doping Content in $\text{Y}_{1-x}\text{Sb}_x\text{Ba}_2\text{Cu}_3\text{O}_{7-d}$ superconductors, *Journal of Magnetism and Magnetic Materials*, (2001), 226-230, 296-297.
- [8] Elsabawy, K. M., Raman Spectra, Microstructure and superconducting properties of Sb(III)-YBCO Composite Superconductor, *Physica C*, (2005), 432, 263-269.
- [9] Azhan, H., Fariesha, F., Yusainee, S. Y. S., Azman, K., & Khalida, S., Superconducting Properties of Ag and Sb Substitution on Low-Density $\text{YBa}_2\text{Cu}_3\text{O}_8$ superconductor, *Journal of Superconductivity and Novel Magnetism*, (2013), 26, 931-935.
- [10] Vezzoli, G.C, Chen, M.F, Graver, F., Katz, R. N., *Materials Science Studies of High-Temperature Superconducting Ceramic Oxides*, Army Research Laboratory, (1997).
- [11] Wu, X. S., Wang, F. Z., Nie, S., Liu, J. S., Yang, L., Jiang, S. S., Structure and Superconductivity in $\text{YBa}_2\text{Cu}_3\text{O}_y$ with Additives of NaNO_3 and NaCl , *Physica C*, (2000), 339, 129-136.
- [12] Akyüz, G. B., Kocabaş, K., Yıldız, A., Özyüzer, L., Çiftçioğlu, M., The Effects of Sb Substitution on Structural Properties in $\text{YBa}_2\text{Cu}_3\text{O}_7$ Superconductors, *Journal of Superconductivity and Novel Magnetism*, (2011), 24, 2189-2201.
- [13] Halim, S. A., Mohamed, S., B, Azhan, H., Khawaldeh, S. A., Sidek, H. A. A., Effect of barium doping in Bi-Pb-Sr-Ca-Cu-O ceramics superconductors, *Physica C Superconductivity*, (1999), 312, 78-84.
- [14] Gokhfeld, D. M., Balaev, D. A., Popkov, S. I., Shaykhutdinov, K. A., Petrov, M. I., Magnetization Loop and Critical Current of Porous Bi-Based HTS, *Physica C*, (2006), 434, 135-137.
- [15] Petrov, M.I., Tetyueva, T.N., Kveglis, L.I., Efremov, A.A., Zeer, G.M., Shaihutdinov, K.A., Balaev, D.A., Popkov, S.I., Ovchinnikov, S.G., Synthesis, Microstructure, and the Transport and Magnetic Properties of Bi-Containing High-Temperature Superconductors with a Porous Structure, *Technical Physic Letter*, (2003), 29, 986-988.